

Regeneration of potassium poisoned catalysts for the selective catalytic reduction of NO with NH₃

Shaojun Liu^{1,2}, Peidong Ji¹, Dong Ye¹, Ruiyang Qu¹, Chenghang Zheng¹, Xiang Gao^{1,*}

¹ State Key Laboratory of Clean Energy Utilization, Zhejiang University, Hangzhou 310027, China

² Key Laboratory of Low-grade Energy Utilization Technologies and Systems (Chongqing University), Ministry of Education of China, Chongqing University, Chongqing 400044, China

* Corresponding author. Tel: 1-350-571-1887; Fax: 1-350-571-1887

E-mail address: xgao1@zju.edu.cn

Abstract

In this study, we investigated the effect of potassium on the activity of the SCR catalysts and the regeneration of potassium-poisoned SCR catalysts. Given the addition of potassium species, NO conversion of catalysts continuously decreased. After washing with H₂SO₄ solution or addition of CeO₂, activities of poisoned catalysts were improved to different extents. For acid washing, surface potassium species were almost completely removed, which made occupied acidic sites be released for the adsorption of NH₃. However, acid washing may also remove part of active components such as vanadia. For CeO₂ doping, extra active components were added. Combined with these two methods, poisoned catalysts were washed with H₂SO₄ solution and then doped with 5 wt.% CeO₂. It was found that the activity could be restored to the level of the fresh one and over 90% NO conversion could be observed between 300 and 450 °C. This is because added CeO₂ compensated the lost active components for the SCR reactions. Consequently, the above hybrid method showed potential application in the regeneration of commercial SCR catalysts.

Keywords: Selective catalytic reduction; Potassium; Deactivation; Regeneration; Ceria.

35 INTRODUCTION

36

37 The selective catalytic reduction (SCR) of NO_x with NH_3 has been regarded as an
38 effective method to control NO_x emissions from stationary and mobile sources (Busca
39 et al., 1998). The commercial SCR catalysts consist of TiO_2 as support and
40 $\text{V}_2\text{O}_5\text{-WO}_3$ or $\text{V}_2\text{O}_5\text{-MoO}_3$ as active components. They are shaped into honeycomb
41 matrix because of the advantages such as low pressure drop, high geometric surface
42 area, and resistance to deposition of dust (Lei et al., 2009).

43 The (co-)firing of biomass is a significant way to reduce the net CO_2 emissions.
44 However, high levels of alkali and alkali earth metals, especially potassium are
45 present in the fly ash of the biomass fired systems. And potassium has been
46 demonstrated to do harm to the SCR catalysts (Kamata et al., 1999; Moradi et al.,
47 2003; Zheng et al., 2004, 2005; Due-Hansen et al., 2007; Castellino et al., 2009;
48 Klimczak et al., 2010). Doping with alkaline and alkaline earth metals results in a
49 strong catalyst deactivation and the poisoning effect of alkali and alkali earth is
50 related to their basicity. The order is listed as $\text{K} > \text{Na} > \text{Ca} > \text{Mg}$ (Klimczak et al.,
51 2010). It is concluded that potassium preferentially coordinates to the Brønsted acid
52 sites, which are responsible for the ammonia adsorption, thus decreasing their number
53 and strength of the Brønsted acid sites. As a result, catalyst activity would be
54 adversely affected. A deactivation of about 1% per day was found over monolith
55 catalysts, which were exposed in a high-dust flue gas produced from straw-fired grate
56 boiler (Zheng et al., 2005).

57 The cost of the catalysts is a major part of the total expense in a SCR system.
58 Hence, it is important and necessary to regenerate the catalysts. Regeneration by
59 washing with water followed by sulfation was not an optimal regeneration method
60 due to the insufficient removal of the poison (Zheng et al., 2004). Washing with
61 sulfuric acid can remove potassium accumulated on the surface and recover the
62 catalytic activity (Khodayari and Odenbrand, 2001b, a; Zheng et al., 2004). However,
63 active components such as vanadium and tungsten can also be removed through
64 washing with sulfuric acid. So, it is necessary to compensate the loss of the active
65 components. Recently, ceria-based catalysts have been investigated for SCR reactions
66 because of the high oxygen storage capacity and excellent redox properties of CeO₂
67 (Chen et al.; Jiang et al.; Li et al., 2012; Hu et al., 2017; Huang et al., 2017; Jiang et
68 al., 2017; Li et al., 2017; Yao et al., 2017). We could also add ceria on the catalyst to
69 compensate the loss of the active components.

70 In this work, potassium ions was doped on the commercial V₂O₅-WO₃/TiO₂
71 catalysts to simulate the poison effect. Then, a study of the regeneration of
72 K-poisoned catalysts was presented. Specifically, loading different amount of ceria on
73 the deactivated catalysts with or without sulfuric acid and deionized water washing
74 have been investigated to show the commercial potential of ceria-involved
75 regeneration method.

76

77 **METHODS**

78

79 **Catalysts preparation**

80 The commercial honeycomb-type catalysts used in this investigation were obtained
81 from RAGA Technology Co., Ltd. The catalysts contained about 1% V_2O_5 and 5%
82 WO_3 as active phase doped on a TiO_2 support. The catalyst had a wall thickness of
83 1mm and a channel pitch of 6 mm. The catalysts were cut into $25\text{mm} \times 20\text{mm} \times$
84 20mm blocks for poisoning of potassium and regeneration method tests.

85 **Deactivating of catalysts**

86 The catalysts doped with potassium were prepared by wet-impregnation method
87 with aqueous solutions of KNO_3 . The prepared monolithic catalysts were immersed
88 into 25ml aqueous solutions with different concentration of KNO_3 . Then the samples
89 were first dried at $110\text{ }^\circ\text{C}$ overnight and then calcined at $500\text{ }^\circ\text{C}$ for 5 h in a muffle
90 furnace to form potassium oxide.

91 **Regeneration of deactivated catalysts**

92 Several blocks of deactivated catalysts (25mm long monolithic segment) were
93 washed in 1000 ml 0.5 M sulfuric acid(SA) solution for 120 min and then washed in
94 1000 ml deionized water for 15 min. In some cases, different concentrations of
95 sulfuric acid (0.05 M, 0.1 M, 0.3 M, 0.5 M, 0.7 M) were used to optimize the washing
96 process. The washing process was under continuous stirring. The temperature of the
97 washing solution was kept at $50\text{ }^\circ\text{C}$. After washing, different contents of CeO_2 were
98 loaded on the catalysts using the same method as potassium doping. Another
99 regeneration method was that CeO_2 was added on the deactivated catalysts without
100 washing process. The catalysts were denoted as $xK-ySA-zCeO_2$. x represents the

101 loading of potassium element (wt. %), y represents the concentration of SA(sulfuric
102 acid) used for catalysts washing(M) and z represents the loading of CeO₂ (wt. %) on
103 the catalysts.

104 **Activity tests**

105 The activity tests for the reduction of NO by NH₃ were carried out in a fixed bed
106 quartz micro-reactor (inner diameter 4 mm) with 0.2 g catalyst power of 250-380 μm
107 in diameter. The feed gas mixture contained 1000 ppm NO, 1000 ppm NH₃, 5 vol. %
108 O₂ and N₂ as the balance gas. The total flow rate of the feed gas was 1000 mL/min
109 and the GHSV was 183000 h⁻¹. The catalytic reaction was carried out with
110 temperature ranging from 150 °C to 450 °C. The concentrations of NO and N₂O
111 before and after reaction were measured by an FTIR gas analyzer Gaset
112 Dx4000. The NO conversion is defined as

$$113 \quad \text{NO Conversion (\%)} = \frac{\text{NO}_{in} - \text{NO}_{out}}{\text{NO}_{in}} \times 100 \quad (1)$$

114 where NO_{in} and NO_{out} stand for the NO concentration at the inlet and outlet,
115 respectively.

116 **Catalyst characterization**

117 The specific surface area and the textural properties (i.e. pore volume and average
118 pore diameter) were measured by N₂ adsorption and desorption experiments at liquid
119 nitrogen temperature (-196°C) with Autosorb-1-C instrument (Quantachrome
120 Instrument Corp.). The specific surface area was calculated by the Brunauer–Emmett–

121 Teller (BET) method while the average pore diameter was calculated from the surface
122 area and BET pore volume.

123 The X-ray diffraction (XRD) patterns were collected using a Panalytical X'pert Pro
124 diffractometer equipped with Cu Ka radiation. The X-ray tube was operated at 40kV
125 and 40mA.

126 The chemical composition of catalyst samples were analyzed by inductively
127 coupled plasma-mass spectroscopy (ICP-MS, model Agilent 7500a) after the catalysts
128 dissolved completely.

129 NH₃-TPD tests were carried out on an AutoChem 2920 instrument provided by
130 Micromeritics Corporation. NH₃ signal was detected using a Hiden QIC20 mass
131 spectrum instrument. 0.2 g catalyst powder was pretreated in He at 500 °C for 30 min.
132 After that, the sample was cooled to 100 °C and exposed to a gas mixture of 5% NH₃
133 in He for 30 min. Then the sample was flushed with pure He until signal was
134 stabilized. The sample was then heated up to 700 °C at a rate of 10 °C/min.

135 H₂-TPR was also carried out in a quartz-tube reactor. 0.10 g catalyst powder was
136 pre-treated at 200 °C in N₂ for 30 min. After that, the sample was cooled to room
137 temperature and then heated to 700 °C at a rate of 10 °C/min in a gas mixture of 5
138 vol.% H₂ and Ar. The consumption of H₂ was detected by a thermal conductivity
139 detector (TCD).

140

141 **RESULTS AND DISCUSSION**

142

143 **Activity and selectivity**

144 Effect of potassium poisoning

145 Fig. 1 shows the activity of the fresh and potassium-loaded catalysts. For the fresh
146 catalyst, the NO conversion increased as the temperature increased, which almost
147 reached 100% at 350 °C. Given that potassium was introduced, the NO conversion
148 decreased. With the increase in the doping amount of potassium, catalyst activity
149 continuously decreased. When the potassium loading amount reached 1%, the NO
150 conversion of the catalyst was always below 30%. This is consistent with the result of
151 Chen et al (Chen et al., 2011).

152 Effect of acid washing

153 To regenerate the poisoned catalyst, the first step is to remove the accumulated K.
154 Sulphuric acid was used as detergent combined with fresh water rinsing after the
155 process. Different concentrations of sulphuric acid solutions were chosen and effect
156 on NO conversion is depicted in Fig.2. It is clear that with concentrated acid,
157 poisoned catalyst is easily recovered, approaching its initial state. However, this effect
158 was gradually weakened when the concentration increased from 0.05 M to 0.5 M.
159 Specially, no obvious difference was observed for the catalysts treated with 0.5 M and
160 0.7 M H₂SO₄. As a result, 0.5 M H₂SO₄ was used in later section for acid washing.
161 Moreover, the washing process also contributed to loss of active components, such as
162 V and W. The negative effect of acid washing is shown in Fig.1s in supporting
163 information. The effect of washing time was also evaluated. It is evident that using
164 diluted acid and short time could remove most of K and reduce the loss of V.
165 However, as shown in Fig.2, the diluted acid washing is hard to totally recover the
166 activity of the catalyst. In another hand, after 2 h washing with 0.5 M H₂SO₄, 40% V

167 of the catalyst was dissolved into the solution, resulting in the reduction of the activity,
168 especially in lower temperatures ($<350\text{ }^{\circ}\text{C}$). For this reason, it is necessary to load
169 active components to compensate the loss.

170 Effect of CeO_2 loading

171 The NO conversion of the K-poisoned and regenerated catalysts is presented in Fig.
172 3. The direct loading of 10% CeO_2 to the deactivated catalyst could improve the
173 activity, which was, however, much lower than that of the fresh catalyst. This is
174 because potassium still remained on the catalyst and exerted a negative effect on the
175 catalyst. Thus, removing potassium species constituted the first step to recover the
176 activity of the deactivated catalyst. After washing with H_2SO_4 solution, an obvious
177 enhancement in the high-temperature activity could be obtained, while the activity
178 below $300\text{ }^{\circ}\text{C}$ remained almost unchanged. It should be noted that the activity of the
179 regenerated catalyst washed with H_2SO_4 solution was still lower than that of the fresh
180 one. That might be due to the loss of active components during the H_2SO_4 solution
181 washing process. Therefore, various amounts of CeO_2 were added to the deactivated
182 catalysts after treatment by $0.5\text{ M H}_2\text{SO}_4$ and deionized water. The NO conversion of
183 $0.5\text{ K-}0.5\text{SA-}3\text{CeO}_2$ catalyst is almost the same as that of the $0.5\text{ K-}10\text{CeO}_2$ catalysts
184 below $300\text{ }^{\circ}\text{C}$. With temperature increasing, $0.5\text{ K-}0.5\text{ SA-}3\text{CeO}_2$ catalyst exhibited a
185 better activity than that of $0.5\text{ K-}10\text{CeO}_2$ catalyst. When the loading amount of CeO_2
186 exceeded 5 wt.%, the activity of the regenerated catalysts almost restored to the level
187 of the fresh one. Thus, it seems that washing with 0.5 M sulfuric acid solution and
188 deionized water and then doping with 5 wt.% CeO_2 is a good method to regenerate the
189 K-poisoned catalysts.

190 In order to investigate the adaptability of this regeneration method, catalyst with a
191 higher potassium loading amount were chosen and tested. As illustrated in Fig. 4, it

192 can be concluded that the amount of potassium had no obvious effect on the activity
193 of the regenerated catalysts in the investigated range and the activity of the
194 regenerated catalysts is almost the same as that of the fresh one. This indicated that
195 0.5M H₂SO₄ and deionized water treatment could remove potassium species that
196 interacted with the active sites, and 5 wt. % CeO₂ additives could supply extra active
197 sites to some extent.

198 Selectivity of regenerated catalysts

199 In addition to NO conversion, N₂O formation is also an important parameter to
200 evaluate catalyst performance. Fig. 5 displays N₂O formation in the SCR reactions.
201 For the fresh and regenerated catalysts, the N₂O concentration were fairly low (< 5
202 ppm) below 350 °C. As the temperature increased, N₂O concentration of the fresh
203 catalyst rapidly increased up to 47 ppm at 450 °C, while the N₂O formation of the
204 regenerated catalysts stayed below 17 ppm, suggesting a better selectivity than the
205 fresh one. This phenomenon could be explained by the reduction of V and the add of
206 Ce, confirmed by Fig.1s and Table 1. Since V₂O₅ has a strong ability to oxidize NH₃
207 into N₂O at higher temperatures(Chen et al., 2009), decrease of V₂O₅ could weaken
208 this side reaction and improve the selectivity of SCR reaction.

209 **Characterization of the catalysts**

210 Chemical composition and BET Analysis

211 Table 1 shows the ICP-MS and BET results of the fresh and regenerated catalysts.
212 It seems that no obvious variations could be observed in these catalysts, partly ruling
213 out the possibility that physical properties mainly determined the activity of the
214 catalysts. Instead, the variations in the chemical properties including acidity and redox
215 constituted the main reason for enhanced activity of the catalysts after regeneration.

216 The ICP-MS results showed that the washing process could drastically remove
217 potassium species over catalyst surface. At the same time, vanadia, as the active
218 component, was also removed a third with the content of tungsten remaining almost
219 unchanged after the washing process. Additionally, the measured Ce content was
220 lower than the calculated value. This meant that there was loss of Ce during
221 impregnation process.

222 XRD analysis

223 XRD patterns of the series catalysts are shown in Fig. 6. All the catalysts presented
224 anatase TiO_2 phase with the absence of V_2O_5 and WO_3 crystallites, indicating that
225 V_2O_5 and WO_3 were amorphous in structure on the TiO_2 support (Lisi et al., 2004;
226 Kustov et al., 2005; Zhang et al., 2009). Given the addition of 3% CeO_2 , no cubic
227 CeO_2 phase could be detect. This result indicated that ceria were highly dispersed and
228 existed as an amorphous state. Further increasing the CeO_2 loading amount to 5% or
229 more, cubic CeO_2 phase began to be observed, suggesting that CeO_2 loading was
230 beyond the theoretical monolayer coverage on the TiO_2 support.

231 NH_3 -TPD

232 According to previous studies, acidity plays an important role in the SCR reactions,
233 since the first step is the adsorption of NH_3 on the surface acidic sites of catalyst
234 (Busca et al., 1998; Forzatti, 2001; Ye et al., 2018). NH_3 -TPD tests were carried out
235 to investigate surface acidity of the series samples, and the results of which are
236 illustrated in Fig. 7. The 0.5K and 0.5K-10 CeO_2 catalysts had several NH_3 desorption
237 peaks in the temperature region of 100-350 °C, while the other catalysts possessed
238 broad desorption peaks between 100 and 450 °C. The peaks near 170 °C (peak I)
239 could be assigned to the desorption of physisorbed NH_3 , and the peaks around 270 °C
240 (peak II) were attributed to NH_3 on weakly acidic sites, while the peaks centering at

241 610 °C(peak III) linked to the strongly acidic sites (Guan et al., 2011; Li et al., 2012;
242 Li et al., 2017; Yao et al., 2017). The quantity analysis of NH₃-TPD is summarized in
243 Table 2. For the 0.5K and 0.5K-10CeO₂ catalysts, the presence of potassium caused
244 the reduction of peak II, which correlated with acidic sites, responsible for SCR
245 activity(Forzatti, 2001). After washing process, abundant acidic sites were present,
246 and NH₃ could be adsorbed on the catalyst surface, reacting with NO. Besides, doping
247 CeO₂ could also in part enhance the acidity of the catalysts, which made
248 0.5K-0.5SA-5CeO₂ catalyst had the same activity with the fresh one (Shi et al., 2017).
249 That is consistent with SCR activity results in Fig.3. Note that after washing and CeO₂
250 modification, peak I increased almost up to two times while peak II reached about
251 80% of that of the fresh catalyst. It may be related to promoted SCR activity at low
252 temperatures and inhibited NH₃ oxidation at high temperatures.

253 H₂-TPR

254 The redox properties of the catalysts play an important role in the catalytic cycle of
255 the SCR reactions (Topsoe, 1994; Topsoe et al., 1995; Putluru et al., 2009; Wang et
256 al., 2018). The H₂-TPR profiles and quantity analysis are shown in Fig. 8 and Table 2,
257 respectively. The fresh catalyst showed a reduction peak located at 500 °C, while the
258 0.5K sample presented a peak at 523 °C. These peaks could be explained by the
259 reduction of V⁵⁺ to V³⁺ (Tang et al., 2010; Chen et al., 2011; Guan et al., 2011). And
260 it should be noted that the reduction peak shifted to higher temperatures after doping
261 potassium, which is consistence with the results of Chen et al (Chen et al., 2011),
262 showing that potassium doping exerted a negative on the catalyst redox properties.
263 After H₂SO₄ washing process, a reduction peak at 485 °C came out. This meant that
264 washing with sulfuric acid solution and deionized water could remove potassium
265 species and recover the redox ability of the catalysts. The reduction peaks shifted to

266 higher temperature with the increasing loading amount of CeO₂. Moreover, the adding
267 of CeO₂ slightly increased the consumption of H₂, compared to 0.5K-0.5SA. This
268 indicated that loading more Ce had a negative effect on the catalyst reducibility.
269 Besides, XPS results shown in Fig.2s confirmed that no obvious change in chemical
270 state of V , W and Ti after acid washing or CeO₂ modification. Combined with
271 aforementioned results, it implied that improved SCR activity after acid washing and
272 CeO₂ adding could be ascribed to optimized acidic sites, which facilitate the low
273 temperature SCR activity and inhibit high temperature NH₃ oxidation.

274

275 **CONCLUSIONS**

276

277 In this study, a new SCR catalyst regeneration method has been developed. Some
278 conclusions are listed below.

279 1. Potassium doping had a negative effect on the activity of the catalysts. The
280 increase in the potassium loading amount continuously decreased the NO conversion
281 of the catalysts. After washing with H₂SO₄ solution and deionized water, SCR activity
282 could be partially restored. Further addition of CeO₂ made the regenerated catalysts
283 possess almost the same activity with the fresh one.

284 2. After washing with H₂SO₄ solution and deionized water, potassium species could
285 be almost completely removed, making occupied acidic sites be released for
286 adsorption of NH₃. Besides, CeO₂ was added for the compensation of the lost active
287 species. These factors constituted the main reasons for the recovery of the catalyst
288 activity after regeneration.

289

290 **ACKNOWLEDGMENTS**

291

292 This work is supported by the National Key Research and Development Program of
293 China (No. 2018YFC0213400), and National Science Foundation of China (NO.
294 U1609212 and NO. 51306079), and Open Fund of Key Laboratory of Ministry of
295 Education of China (No. LLEUTS-201507).

296

297 **DISCLAIMER**

298

299 Reference to any companies or specific commercial products does not constitute.

300

301 **REFERENCES**

302

303 Busca, G., Lietti, L., Ramis, G. and Berti, F. (1998). Chemical and Mechanistic
304 Aspects of the Selective Catalytic Reduction of NO_x by Ammonia over Oxide
305 Catalysts: A Review. *Appl. Catal. B-Enviro.* 18: 1-36.

306 Castellino, F., Jensen, A.D., Johnsson, J.E. and Fehrmann, R. (2009). Influence of
307 Reaction Products of K-Getter Fuel Additives on Commercial Vanadia-Based SCR
308 Catalysts Part I. Potassium Phosphate. *Appl. Catal. B-Enviro.* 86: 196-205.

309 Chen, L., Li, J. and Ge, M. (2009). Promotional Effect of Ce-Doped V₂O₅-WO₃/TiO₂
310 with Low Vanadium Loadings for Selective Catalytic Reduction Of NO_x by NH₃. *J.*
311 *Phys. Chem. C* 113: 21177-21184.

312 Chen, L., Li, J.H. and Ge, M.F. (2011). The Poisoning Effect of Alkali Metals Doping
313 over Nano V₂O₅-WO₃/TiO₂ Catalysts on Selective Catalytic Reduction of NO_x by
314 NH₃. *Chem. Eng. J.* 170: 531-537.

315 Chen, Y., Wang, M., Du, X., Ran, J., Zhang, L. and Tang, D. High Resistance to Na
316 Poisoning of V_2O_5 - $Ce(SO_4)_2/TiO_2$ Catalyst for the NO SCR Reaction. *Aerosol Air*
317 *Qual. Res.*, in press.

318 Due-Hansen, J., Boghosian, S., Kustov, A., Fristrup, P., Tsilomelekis, G., Stahl, K.,
319 Christensen, C.H. and Fehrmann, R. (2007). Vanadia-Based SCR Catalysts
320 Supported on Tungstated and Sulfated Zirconia: Influence of Doping with
321 Potassium. *J. Catal.* 251: 459-473.

322 Forzatti, P. (2001). Present Status and Perspectives in De-NO_x SCR Catalysis. *Appl.*
323 *Catal. A-Gen.* 222: 221-236.

324 Guan, B., Lin, H., Zhu, L. and Huang, Z. (2011). Selective Catalytic Reduction of
325 NO_x with NH₃ over Mn, Ce Substitution $Ti_{0.9}V_{0.1}O_{2-\delta}$ Nanocomposites Catalysts
326 Prepared by Self-Propagating High-Temperature Synthesis Method. *J. Phys. Chem.*
327 *C* 115: 12850-12863.

328 Hu, W., Zhang, Y., Liu, S., Zheng, C., Gao, X., Nova, I. and Tronconi, E. (2017).
329 Improvement in Activity and Alkali Resistance of a Novel V- $Ce(SO_4)_2/Ti$ Catalyst
330 for Selective Catalytic Reduction of NO with NH₃. *Appl. Catal. B-Enviro.* 206:
331 449-460.

332 Huang, X., Ma, Z., Lin, W., Liu, F. and Yang, H. (2017). Activation of Fast Selective
333 Catalytic Reduction of NO by NH₃ at Low Temperature Over TiO_2 Modified
334 CuO_x - CeO_x Composites. *Catal. Commun.* 91: 53-56.

335 Jiang, Y., Bao, C., Liu, S., Liang, G., Lu, M., Lai, C., Shi, W. and Ma, S. Enhanced
336 Activity of Nb-modified CeO₂/TiO₂ Catalyst for the Selective Catalytic Reduction
337 of NO with NH₃. *Aerosol Air Qual. Res.* in press.

338 Jiang, Y., Wang, X., Xing, Z., Bao, C. and Liang, G. (2017). Preparation and
339 Characterization of CeO₂-MoO₃/TiO₂ Catalysts for Selective Catalytic Reduction
340 of NO with NH₃. *Aerosol Air Qual. Res.* 17: 465-469.

341 Kamata, H., Takahashi, K. and Odenbrand, C.U.I. (1999). The Role of K₂O in the
342 Selective Reduction of NO with NH₃ over a V₂O₅(WO₃)/TiO₂ Commercial
343 Selective Catalytic Reduction Catalyst. *J. Mol. Catal. A-Chem.* 139: 189-198.

344 Khodayari, R. and Odenbrand, C.U.I. (2001a). Regeneration of Commercial SCR
345 Catalysts by Washing and Sulphation: Effect of Sulphate Groups on the Activity.
346 *Appl. Catal. B-Enviro.* 33: 277-291.

347 Khodayari, R. and Odenbrand, C.U.I. (2001b). Regeneration of Commercial
348 TiO₂-V₂O₅-WO₃ SCR Catalysts Used in Bio Fuel Plants. *Appl. Catal. B-Enviro.* 30:
349 87-99.

350 Klimczak, M., Kern, P., Heinzelmann, T., Lucas, M. and Claus, P. (2010).
351 High-Throughput Study of the Effects of Inorganic Additives and Poisons on
352 NH₃-SCR Catalysts Part I: V₂O₅-WO₃/TiO₂ Catalysts. *Appl. Catal. B-Enviro.* 95:
353 39-47.

354 Kustov, A.L., Kustova, M.Y., Fehrmann, R. and Simonsen, P. (2005). Vanadia on
355 Sulphated-ZrO₂, a Promising Catalyst for NO Abatement with Ammonia in Alkali
356 Containing Flue Gases. *Appl. Catal. B-Enviro.* 58: 97-104.

357 Lei, Z.G., Liu, X.Y. and Jia, M.R. (2009). Modeling of Selective Catalytic Reduction
358 (SCR) for NO Removal Using Monolithic Honeycomb Catalyst. *Energy Fuels* 23:
359 6146-6151.

360 Li, L., Zhang, L., Ma, K., Zou, W., Cao, Y., Xiong, Y., Tang, C. and Dong, L. (2017).
361 Ultra-Low Loading of Copper Modified TiO₂/CeO₂ Catalysts for Low-Temperature
362 Selective Catalytic Reduction Of NO by NH₃. *Appl. Catal. B-Enviro.* 207: 366-375.

363 Li, Q., Hou, X., Yang, H., Ma, Z., Zheng, J., Liu, F., Zhang, X. and Yuan, Z. (2012).
364 Promotional Effect of CeO_x for NO Reduction over V₂O₅/TiO₂-Carbon Nanotube
365 Composites. *J. Mol. Catal. A-Chem.* 356: 121-127.

366 Lisi, L., Lasorella, G., Malloggi, S. and Russo, G. (2004). Single and Combined
367 Deactivating Effect of Alkali Metals and HCl on Commercial SCR Catalysts. *Appl.*
368 *Catal. B-Enviro.* 50: 251-258.

369 Moradi, F., Brandin, J., Sohrabi, M., Faghihi, M. and Sanati, M. (2003). Deactivation
370 of Oxidation and SCR Catalysts Used in Flue Gas Cleaning by Exposure to
371 Aerosols of High- and Low Melting Point Salts, Potassium Salts and Zinc Chloride.
372 *Appl. Catal. B-Enviro.* 46: 65-76.

373 Putluru, S.S.R., Riisager, A. and Fehrmann, R. (2009). The Effect of Acidic and
374 Redox Properties of V_2O_5/CeO_2-ZrO_2 Catalysts in Selective Catalytic Reduction of
375 NO by NH_3 . *Catal. Lett.* 133: 370-375.

376 Shi, Y., Wang, X., Xia, Y., Sun, C., Zhao, C., Li, S. and Li, W. (2017). Promotional
377 Effect of CeO_2 on the Propene Poisoning Resistance of Hbea Zeolite Catalyst for
378 NH_3 -SCR of NO_x . *Mol. Catal.* 433: 265-273.

379 Tang, F.S., Xu, B.L., Shi, H.H., Qiu, J.H. and Fan, Y.N. (2010). The Poisoning Effect
380 of Na^+ and Ca^{2+} Ions Doped on the V_2O_5/TiO_2 Catalysts for Selective Catalytic
381 Reduction of NO by NH_3 . *Appl. Catal. B-Enviro.* 94: 71-76.

382 Topsoe, N.Y. (1994). Mechanism of the Selective Catalytic Reduction of Nitric-Oxide
383 by Ammonia Elucidated by in-Situ Online Fourier-Transform
384 Infrared-Spectroscopy. *Science* 265: 1217-1219.

385 Topsoe, N.Y., Topsoe, H. and Dumesic, J.A. (1995). Vanadia-Titania Catalysts for
386 Selective Catalytic Reduction (SCR) of Nitric-Oxide by Ammonia .1. Combined
387 Temperature-Programmed in-Situ FTIR and Online Mass-Spectroscopy Studies. *J.*
388 *Catal.* 151: 226-240.

389 Wang, X., Shi, Y., Li, S. and Li, W. (2018). Promotional Synergistic Effect of Cu and
390 Nb Doping on a Novel Cu/Ti-Nb Ternary Oxide Catalyst for the Selective Catalytic
391 Reduction of NO_x with NH_3 . *Appl. Catal. B-Enviro.* 220: 234-250.

392 Yao, X., Zhao, R., Chen, L., Du, J., Tao, C., Yang, F. and Dong, L. (2017). Selective
393 Catalytic Reduction of NO_x by NH₃ over CeO₂ Supported on TiO₂: Comparison of
394 Anatase, Brookite, and Rutile. *Appl. Catal. B-Enviro.* 208: 82-93.

395 Ye, D., Qu, R., Zhang, Y., Wu, W., Liu, S., Zheng, C. and Gao, X. (2018).
396 Investigating the Role of H₄SiW₁₂O₄₀ in the Acidity, Oxidability and Activity of
397 H₄SiW₁₂O₄₀-Fe₂O₃ Catalysts for the Selective Catalytic Reduction of NO with NH₃.
398 *Mol. Catal.* 448: 177-184.

399 Zhang, X., Li, X.G., Wu, J.S., Yang, R.C. and Zhang, Z.H. (2009). Selective Catalytic
400 Reduction of No by Ammonia on V₂O₅/TiO₂ Catalyst Prepared by Sol-Gel Method.
401 *Catal. Lett.* 130: 235-238.

402 Zheng, Y.J., Jensen, A.D. and Johnsson, J.E. (2004). Laboratory Investigation of
403 Selective Catalytic Reduction Catalysts: Deactivation by Potassium Compounds
404 and Catalyst Regeneration. *Ind. Eng. Chem. Res.* 43: 941-947.

405 Zheng, Y.J., Jensen, A.D. and Johnsson, J.E. (2005). Deactivation of V₂O₅-WO₃-TiO₂
406 SCR Catalyst at a Biomass-Fired Combined Heat and Power Plant. *Appl. Catal.*
407 *B-Enviro.* 60: 253-264.

408
409
410
411

412 **Table 1.** Chemical composition, BET surface area, total pore volume, and average
 413 pore diameter of different samples

Sample	Amount (wt %)				Surface area(m ² /g)	Total pore volume(cm ³ /g)	Average pore diameter(nm)
	V	W	K	Ce ^a			
Fresh	0.67	3.72	0.03	0.00	63.3	0.312	19.71
0.5K	0.73	4.16	0.34	-	66.7	0.309	18.55
0.5K-0.5SA	0.44	3.90	0.05	-	62.7	0.346	22.06
0.5K-10CeO ₂	0.61	3.35	0.25	9.54	65.1	0.301	18.48
0.5K-0.5SA-3CeO ₂	0.44	3.90	0.04	1.37	67.5	0.353	20.91
0.5K-0.5SA-5CeO ₂	0.41	3.76	0.04	2.36	65.4	0.330	20.21
0.5K-0.5SA-10CeO ₂	0.39	3.45	0.04	9.24	60.5	0.274	18.09

414 ^a Amount of Ce is from EDS analysis.

415

416

Table 2. Quantitative analysis of NH₃-TPD and H₂-TPR over the samples*.

Samples	Peak		NH ₃		Total NH ₃	Total H ₂
	temperature(°C)		desorption		desorption	consumption
	T _I	T _{II}	(a.u.)		(a.u.)	(a.u.)
			S _I	S _{II}	S _I +S _{II}	
Fresh	178	270	1.00	1.00	1.00	1.00
0.5K	165	236	1.34	0.63	0.74	0.93
0.5K-0.5SA	183	293	1.22	1.05	1.08	0.63
0.5K-10CeO ₂	164	227	1.11	0.40	0.51	1.38
0.5K-0.5SA-3CeO ₂	205	314	1.64	0.73	0.86	0.67
0.5K-0.5SA-5CeO ₂	188	282	2.00	0.87	1.04	0.87
0.5K-0.5SA-10CeO ₂	180	267	1.92	0.81	0.98	0.76

417

*Normalized by the values of the fresh catalyst

418

419

Figure Captions

420

421 **Fig. 1.** NO conversion of the catalysts poisoned with different K loading amounts.

422 **Fig. 2.** NO conversion of the catalysts regenerated with different concentrations of

423 H₂SO₄ solution.

424 **Fig. 3.** NO conversion of the catalysts regenerated with different cerium loading

425 amounts.

426 **Fig. 4.** Effect of K contents on the catalysts regenerated by washing and CeO₂

427 modification.

428 **Fig. 5.** N₂O formation of the catalysts regenerated by washing and CeO₂ modification.

429 **Fig. 6.** XRD patterns of the (a): Fresh; (b): 0.5K; (c): 0.5K-0.5SA; (d): 0.5K-10CeO₂;

430 (e): 0.5K-0.5SA-3CeO₂; (f): 0.5K-0.5SA-5CeO₂; (g): 0.5K-0.5SA-10CeO₂.

431 **Fig. 7.** NH₃-TPD curves of the (a): Fresh; (b): 0.5K; (c): 0.5K-0.5SA; (d):

432 0.5K-10CeO₂; (e): 0.5K-0.5SA-3CeO₂; (f): 0.5K-0.5SA-5CeO₂; (g):

433 0.5K-0.5SA-10CeO₂.

434 **Fig. 8.** H₂-TPR profiles of the (a): Fresh; (b): 0.5K; (c): 0.5K-0.5SA; (d):

435 0.5K-10CeO₂; (e): 0.5K-0.5SA-3CeO₂; (f): 0.5K-0.5SA-5CeO₂; (g):

436 0.5K-0.5SA-10CeO₂.

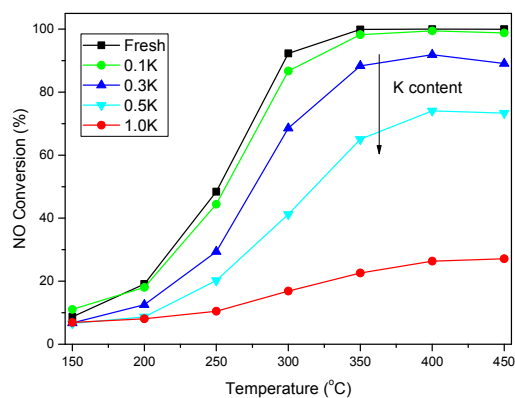
437

438

439

440

441



442

443

444 **Fig. 1.** NO conversion of the catalysts poisoned with different K loading amounts.

445

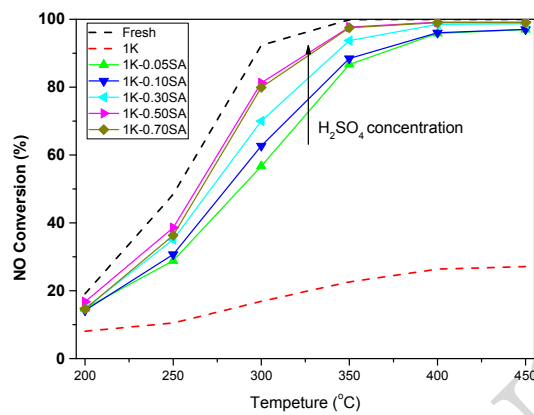
446

447

448

449

450



451

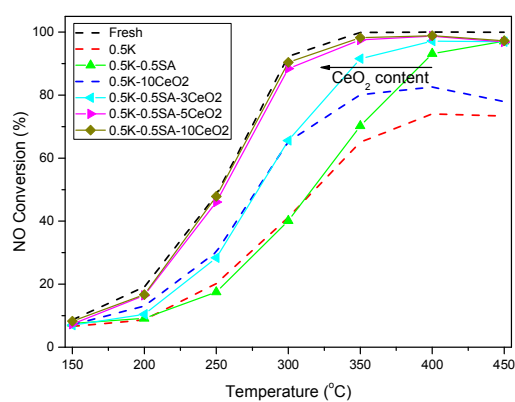
452 **Fig. 2.** NO conversion of the catalysts regenerated with different concentrations of H₂SO₄

453

solution.

ACCEPTED MANUSCRIPT

454



455

456

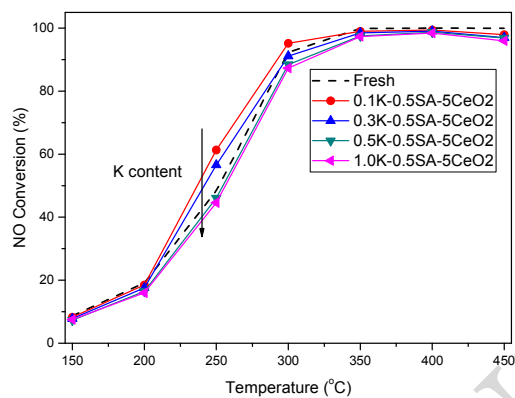
457 **Fig. 3.** NO conversion of the catalysts regenerated with different cerium loading amounts.

458

ACCEPTED MANUSCRIPT

459

460



461

462

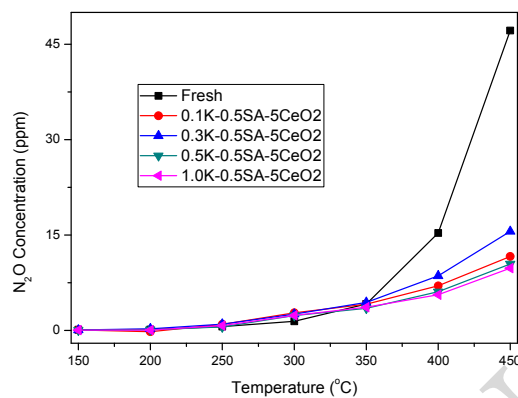
463 **Fig. 4.** Effect of K contents on the catalysts regenerated by washing and CeO₂ modification.

464

ACCEPTED MANUSCRIPT

465

466

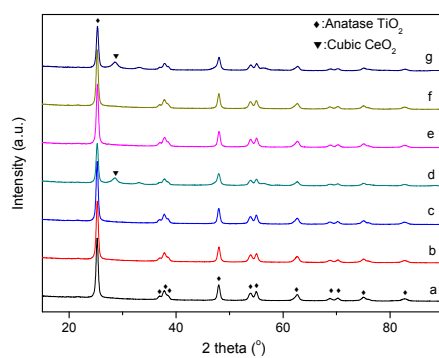


467

468

469 **Fig. 5.** N₂O formation of the catalysts regenerated by washing and CeO₂ modification.

470



471

472 **Fig. 6.** XRD patterns of the (a): Fresh; (b): 0.5K; (c): 0.5K-0.5SA; (d): 0.5K-10CeO₂; (e):

473 0.5K-0.5SA-3CeO₂; (f): 0.5K-0.5SA-5CeO₂; (g): 0.5K-0.5SA-10CeO₂.

474

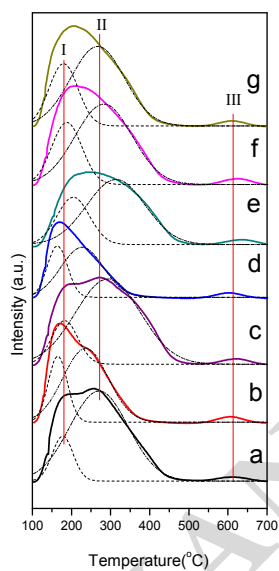
475

476

ACCEPTED MANUSCRIPT

477

478

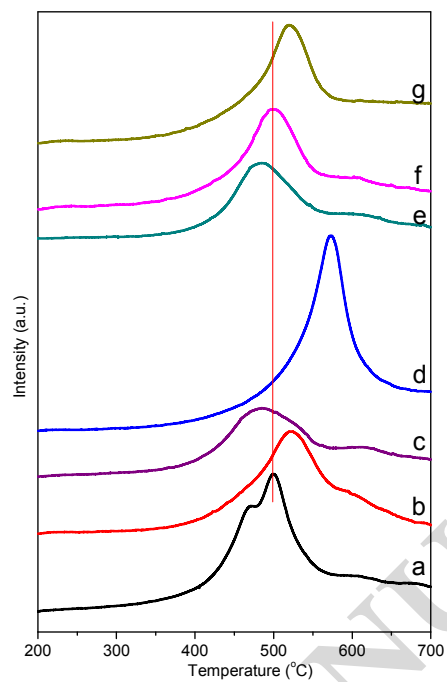


479

480 **Fig. 7.** NH₃-TPD curves of the (a): Fresh; (b): 0.5K; (c): 0.5K-0.5SA; (d): 0.5K-10CeO₂; (e):

481 0.5K-0.5SA-3CeO₂; (f): 0.5K-0.5SA-5CeO₂; (g): 0.5K-0.5SA-10CeO₂.

482



483

484 **Fig. 8.** H₂-TPR profiles of the (a): Fresh; (b): 0.5K; (c): 0.5K-0.5SA; (d): 0.5K-10CeO₂; (e):

485 0.5K-0.5SA-3CeO₂; (f): 0.5K-0.5SA-5CeO₂; (g): 0.5K-0.5SA-10CeO₂.

486

487